Flux observation for the MMS-sponsored project entitled

"METEOROLOGICAL AND WAVE MEASUREMENTS FOR IMPROVING METEOROLOGICAL AND AIR QUALITY MODELING"

Ludovic Bariteau[1], C. W. Fairall[2], Sergio Pezoa[2], Jeff Hare[3]

1 Cooperative Institute for Research in Environmental Sciences (CIRES), University of Colorado

2 NOAA Earth System Research Laboratory (ESRL), Physical Sciences Division

3 Joint Institute for Marine and Atmospheric Research (JIMAR), University of Hawaii

Contact: Ludovic Bariteau, NOAA ESRL R/PSD03, 325 Broadway, Boulder CO 80305-3337, USA. (ludovic.bariteau@noaa.gov)

June, 2012

Table of contents

1) Introduction and Goals

The main goal of this project is to collect meteorological data that can be used to better characterize the atmospheric boundary layer over the Gulf of Mexico. As part of this effort with STi and LSU, the Earth System Research Laboratory (ESRL) Physical Science
Division (PSD) Air-Sea Interaction group and the University of Colorado provided two turbulent flux systems, composed of two sonic anemometers and two LiCOR 7500 that were deployed on the Chevron Platform, ST-52B (also refereed as CSI06). This station is located about 20km (12.4 miles) South of Terrebonne Bay, Louisiana (see Figure 1 below).

In this report, we conduct a limited analysis that compares the COARE algorithm to the eddy-correlation flux measurements. In Section 2, the different suites of instruments used in this study are described. Section 3 shows the analysis procedures used for the study. Results and discussion are provided in Sections 4 to 6. Finally, conclusions are given in Section 5.

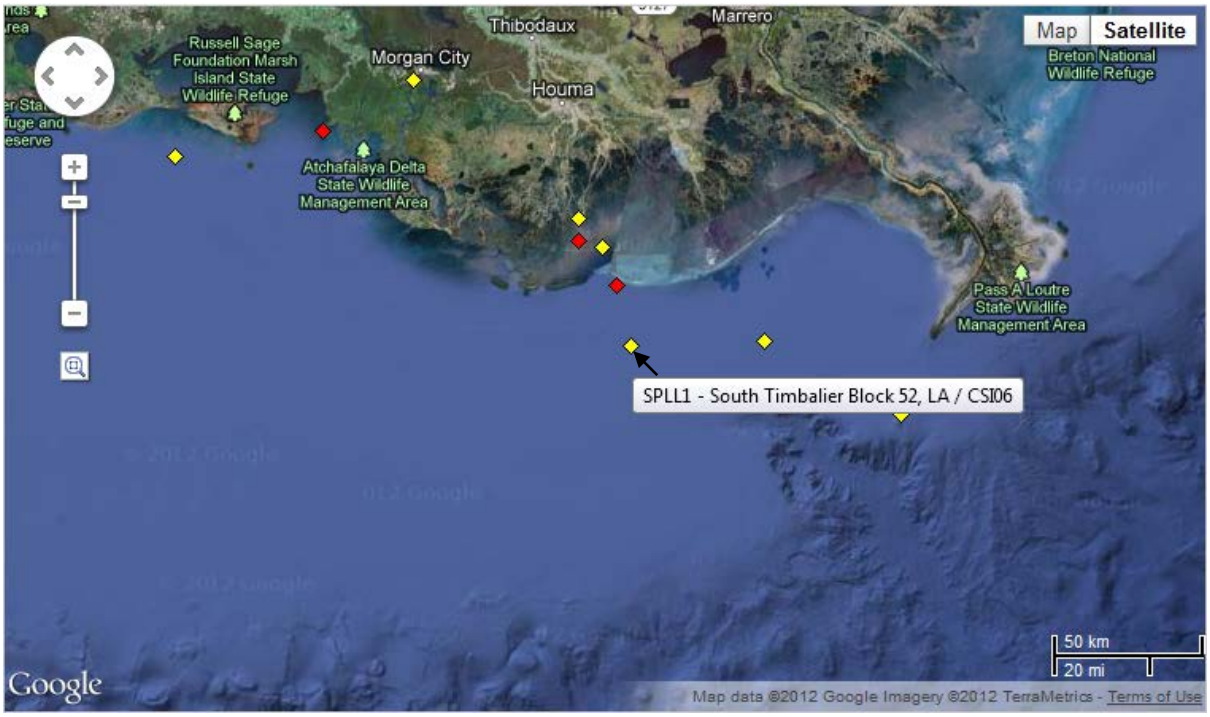

Figure 1. Map from the National Data Buoy Center (NDBC) showing the location of station CSI06 (coordinates: 90º29' W, 28º52' N).

2) Instrumentation description

a) Flux system

The PSD turbulent flux system consists of two sets of components, two ultrasonic anemometer, Gill Wind MasterPro, and two LI-COR 7500 fast CO2/H2O gas analyzers. These flux packages were located on the AB and AC bridges of the platform (see Figures 2 and 3). In what follows, AB refers to the instruments on the AB bridge (i.e. AB sonic), AC to the AC bridge.

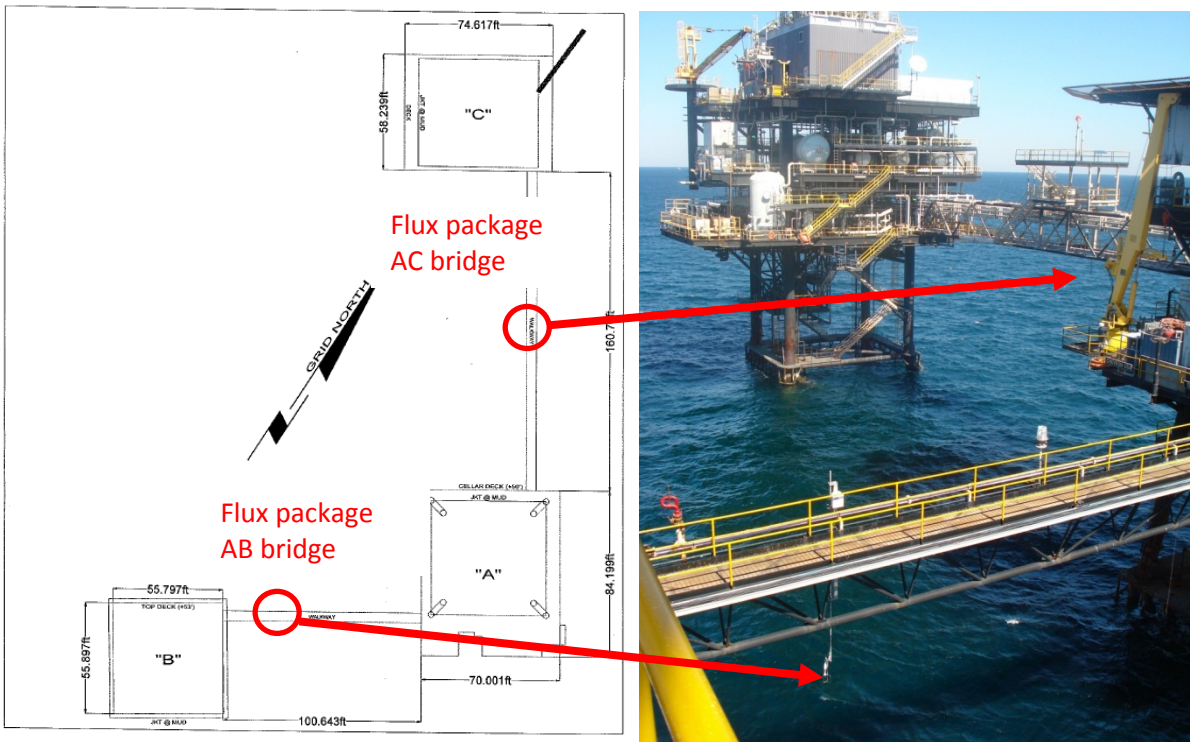

Figure 2. Location of the AB and AC flux packages on the platform.

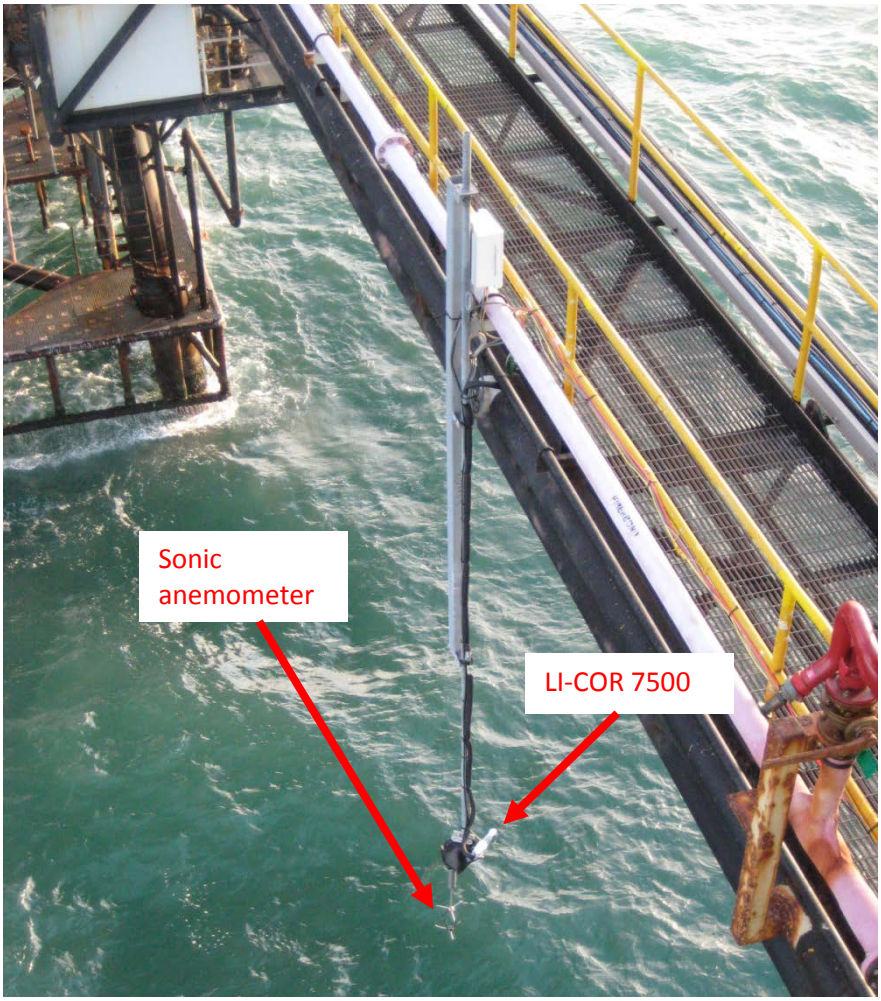

Figure 3. Close-up view of the AB flux package.

The central data acquisition computer continuously logging all sources of data is located in an enclosure close by the AB flux package. Table 1 shows sampling rates and deployment heights of the PSD sensors.

Sensor	Sampling rate (Hz)	Height (m)
AB sonic	10	11
AB Licor	10	11
AC sonic	10	14
AC Licor	10	14

Table 1. Flux package sensor heights and sampling rates.

b) Meteorological system

Meteorological instruments from STi and LSU were also deployed on the top deck of the B structure (Figure 4). These include wind speed and direction, air temperature and humidity, shortwave and longwave observations. The instrument heights and available data rate are described in Table 2. It has to be noted that a rain sensor was also deployed but found not to operate properly in the data made available. In what follows, STI refers to STI's instruments and LSU to LSU's instruments.

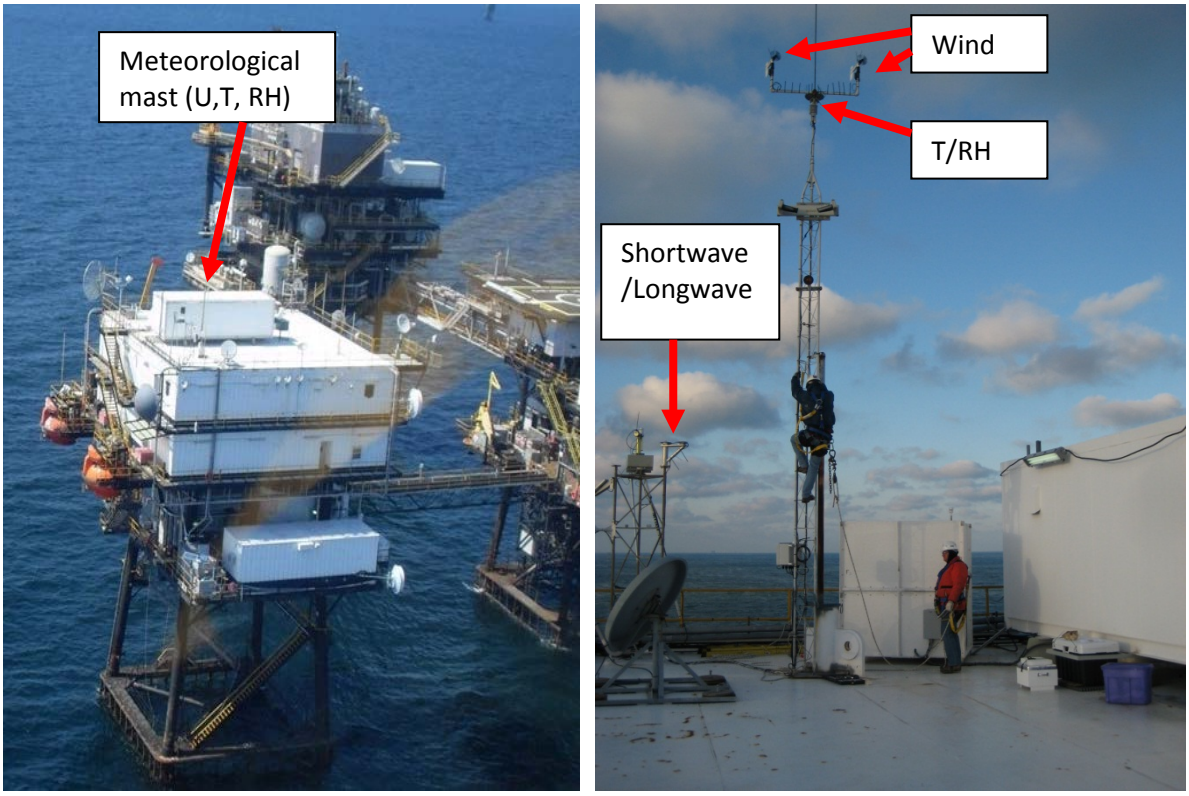

Figure 4. Left: Aerial view of the meteorological observations from the top of the B structure. Right: Close-up view of the 10-m meteorological tower and radiations measurements on top of the B platform.

Sensor	Available data rate	Height (m)
STI Windbird	1-min data	39.98
STI T/RH	1-min data	39.27
LSU T/RH	hourly data	39.57
LSU Windbird	hourly data	39.98
LSU Barometer	hourly data	corrected to sea level
LSU wave sensor	hourly data	-1
STI IR skin SST	1-min data	~30
STI floating thermistor	1-min data	-0.2
STI radiometers	1-min data	~33

Table 2. STI and LSU sensor heights and available data rates.

3) Method

The data used for that comparison are from January 1, 2011 to December 31, 2011. Data from January 1, 2012 to May 5, 2012 were also processed but are not used in that comparison for ease. For illustration, the 10-min average time series of true wind speed, true wind direction (relative to North), air temperature (blue), sea surface temperature (red), incident shortwave (blue) and longwave (red), relative humidity and atmospheric pressure are shown for the year of 2011 and 2012 in Figures 5a and 5b. The data gaps are due to instrument or acquisition system failures. For the meteorological data about 90% of data are available for the year of 2011, while about 72% - 84% of the data exist for the flux packages (AC – AB respectively).

In this study, the following steps were employed:

- covariance fluxes and mean meteorological states were calculated over a 10-min time period. Standard meteorological wind direction was adopted for all of observations and sign convention for fluxes is positive upward, i.e. away from the surface.

- all the sources of meteorological data were compared and evaluated in order to select an ideal dataset to compute fluxes from the COARE algorithm

- covariance fluxes were then quality controlled (QC) via numerous filters (more details below) and then compared against BULK fluxes.

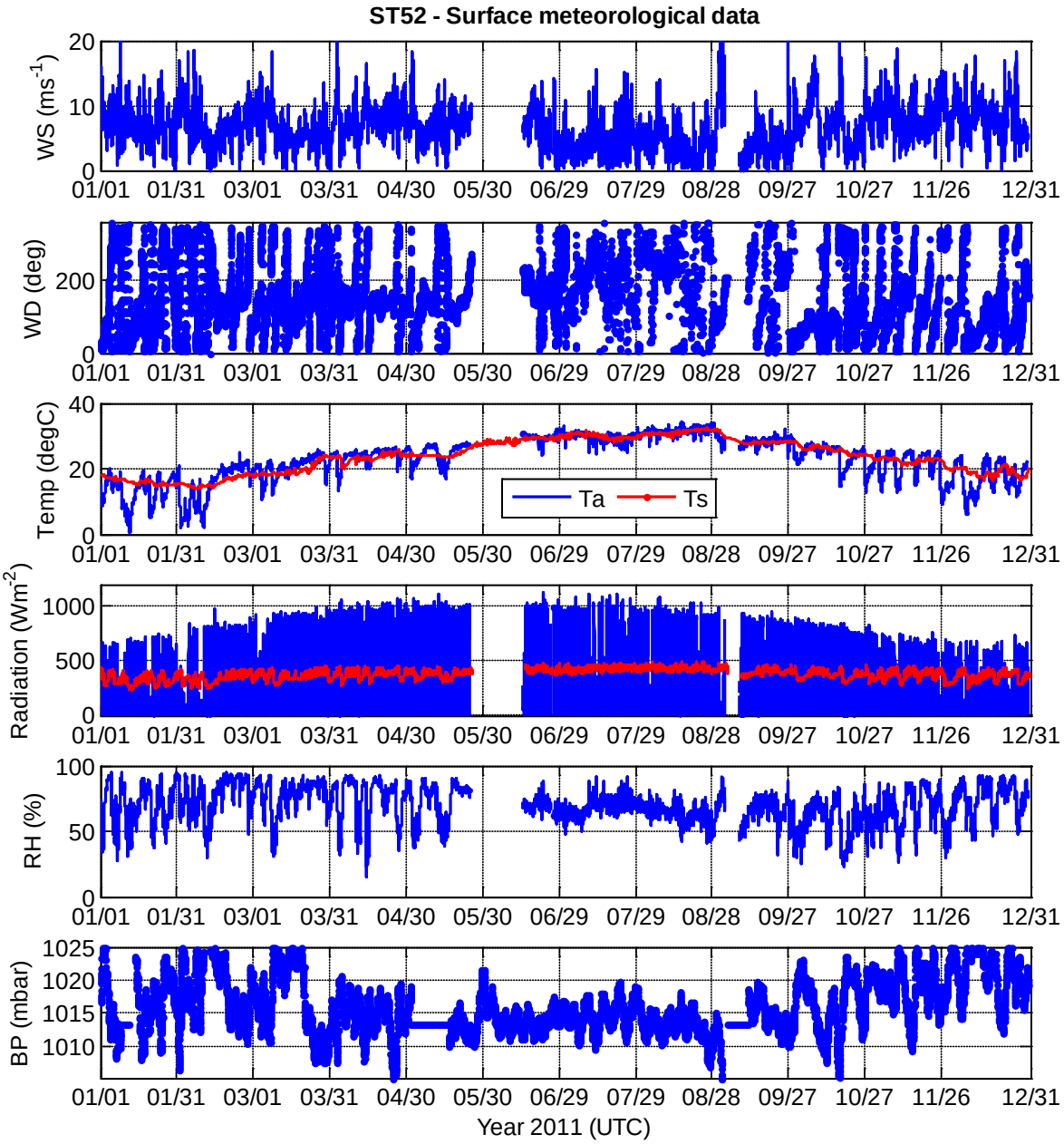

Figure 5a. Meteorological conditions from the platform during year 2011. From the top, the panels show the wind speed (m.s-1), the wind direction in degrees relative to North, the air temperature in blue and SST in red (°C), the incident shortwave (blue) and longwave (red) radiations (W.m-2), the relative humidity (%) and the barometric pressure (mb).

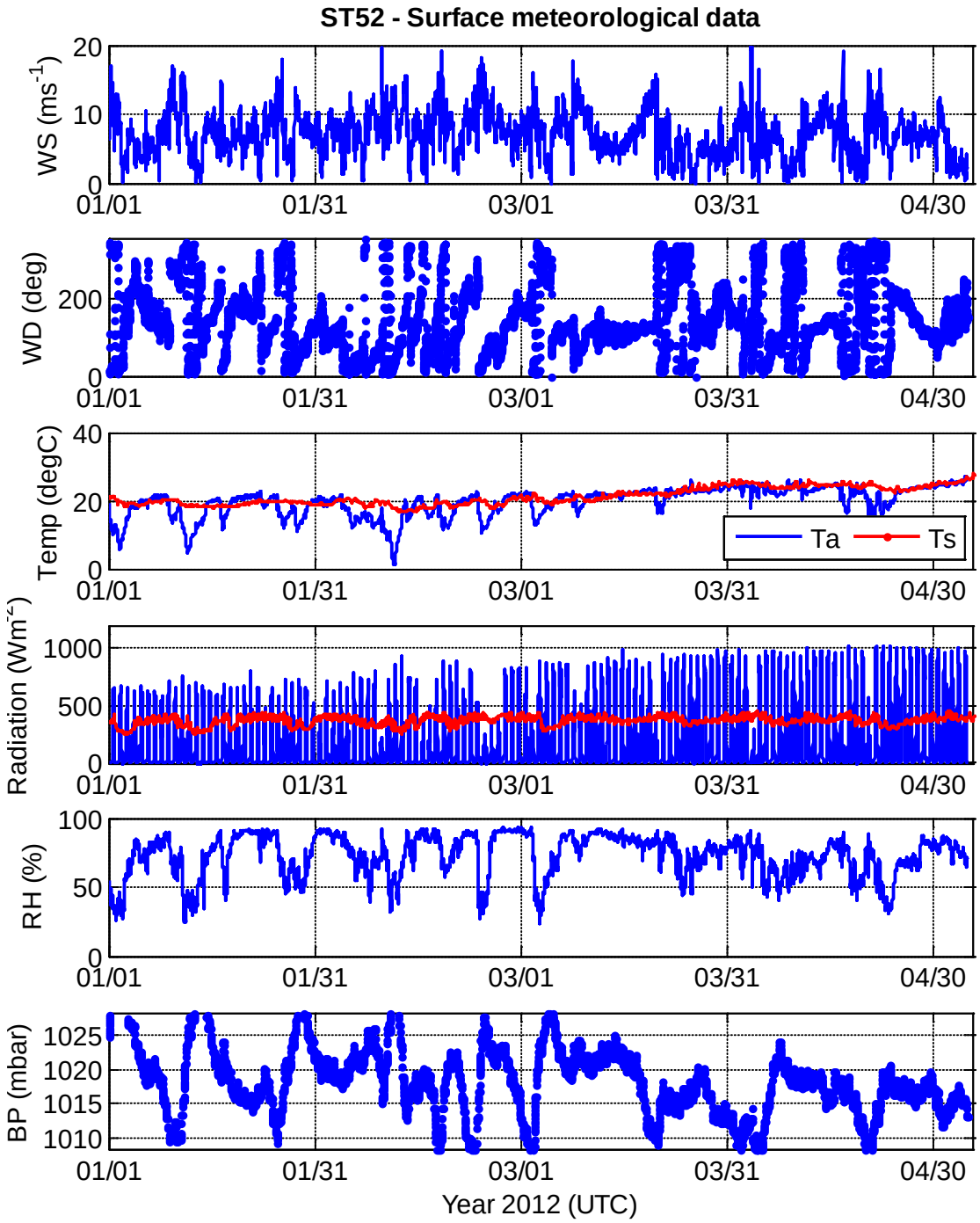

Figure 5b. Meteorological conditions from the platform during year 2012. From the top, the panels show the wind speed (m.s-1), the wind direction in degrees relative to North, the air temperature in blue and SST in red (°C), the incident shortwave (blue) and longwave (red) radiations (W.m-2), the relative humidity (%) and the barometric pressure (mb).

4) Meteorological data evaluation

In this section, we briefly look at the various surface observations available on the platform and try to select what we think might be the best data set with which to run the COARE algorithm.

a) Air temperature

Figure 6 shows time series of air temperature measurements for year 2011. As noted during deployment, the sonic anemometers are offset from one another by about 5 degC. However this should not affect the turbulent fluxes as fluxes are based on the variations instead of the means. We note also that the LSU temperature measurement runs about 1degC lower than the STi unit in the first half of the year, but then measures about 2degC higher after replacement. Because we have no way at that time to know which instrument is correct; we select the STi measurement for the COARE inputs. Post calibration of the two temperature sensor would help reduce this uncertainty.

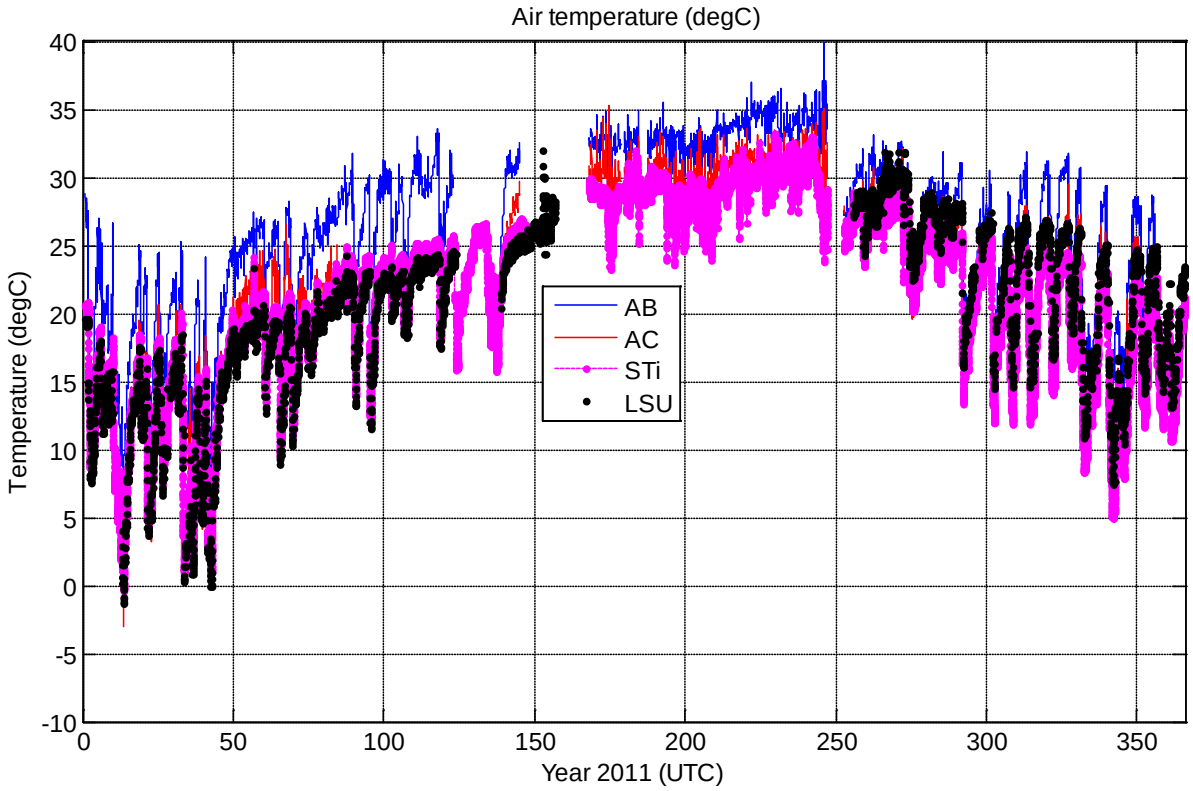

Figure 6. Time series of air temperatures for the two sonic anemometers (blue and red), and the temperature measurements on the B roof (magenta and black).

b) Relative humidity

Figure 7 shows relative humidity measurements from STI and LSU's collocated instruments. We note that LSU instrument behaves abnormally several times prior its replacement in the fall of 2011. As a result, we use the STi measurement for the BULK calculation and note that the STi and LSU units differ by 6% (~3 g/kg) from day 250 to 365. Again a post calibration might help reduce the uncertainty in the BULK latent heat flux.

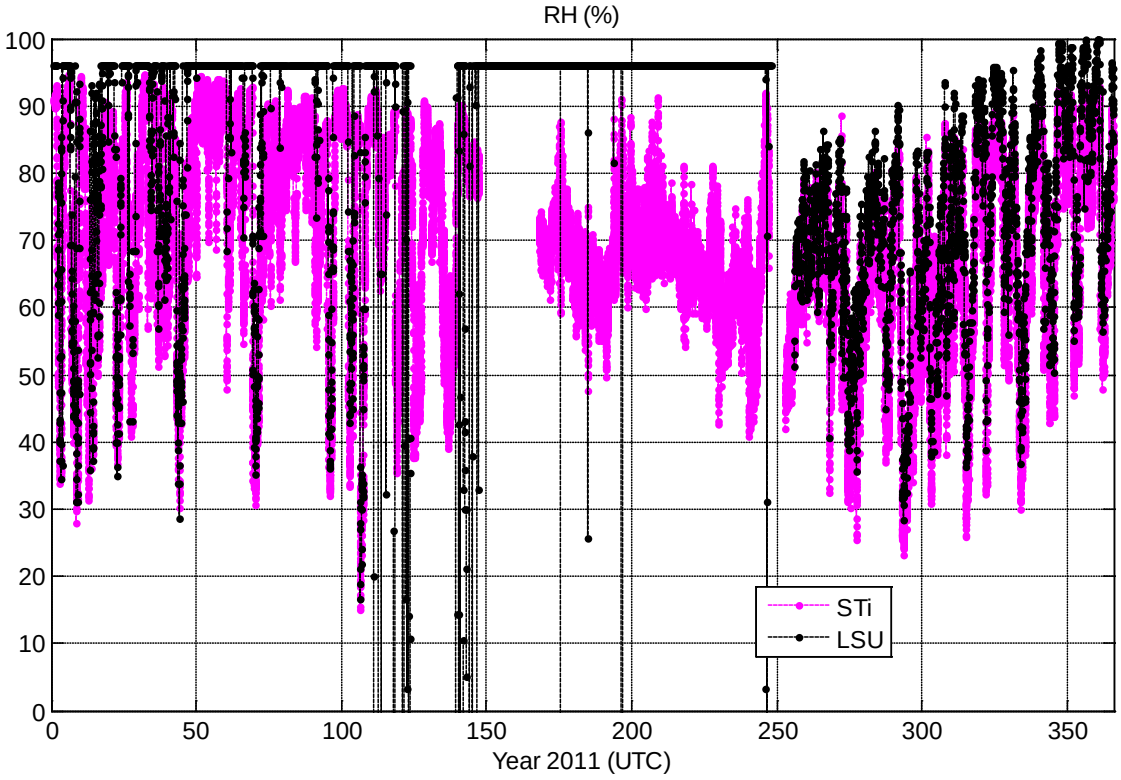

Figure 7. Relative humidity from STI (magenta) and LSU (black).

c) Sea temperature

Figure 8 shows time series of sea temperatures from an instrument at approximately 1 m below mean water level (LSU) and from a floating thermistor (STi) deployed sometimes in July of 2011. At first, the STi and LSU instrument are within .5 degC of each other at night (no corrections applied) but seems to slightly drift apart from each other as time passes by (up to 1degC at night by the end of the year). For the BULK fluxes, we decide to use the LSU instrument (1m) for the first half of the year, and then use the floating thermistor (~20 cm depth) for the second half.

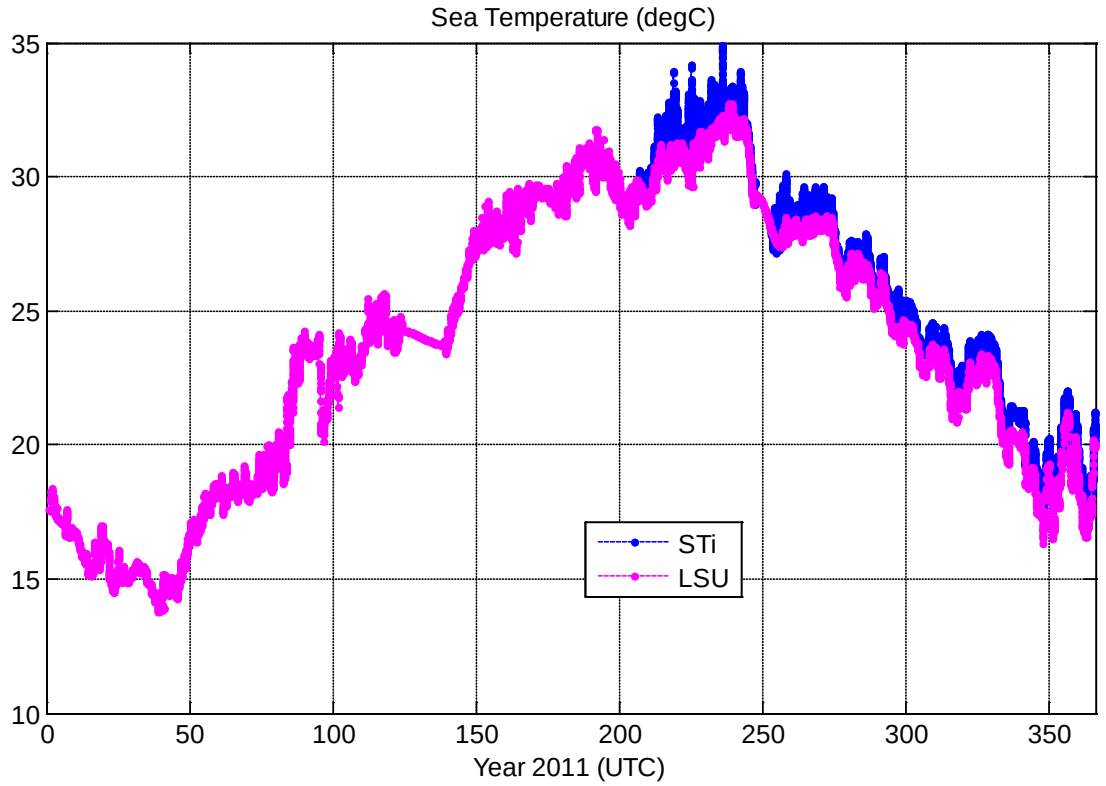

Figure 8. Time series of air and sea temperatures from STI (blue and magenta) and LSU (black and green) instruments.

d) Wind speed and direction

Figure 9 show 10-m wind speed residuals (instrument to compare minus STI wind) as a function of true wind direction. Similarly wind direction residuals as a function of true wind direction are plotted on Figure 10. Both STi and LSU wind speeds are within 0.5 m/s from each other and within 5deg for wind directions. Therefore we will use the STi sensor for the COARE algorithm. We note also various flow distortion effects from the platform. More details are given in the QC section.

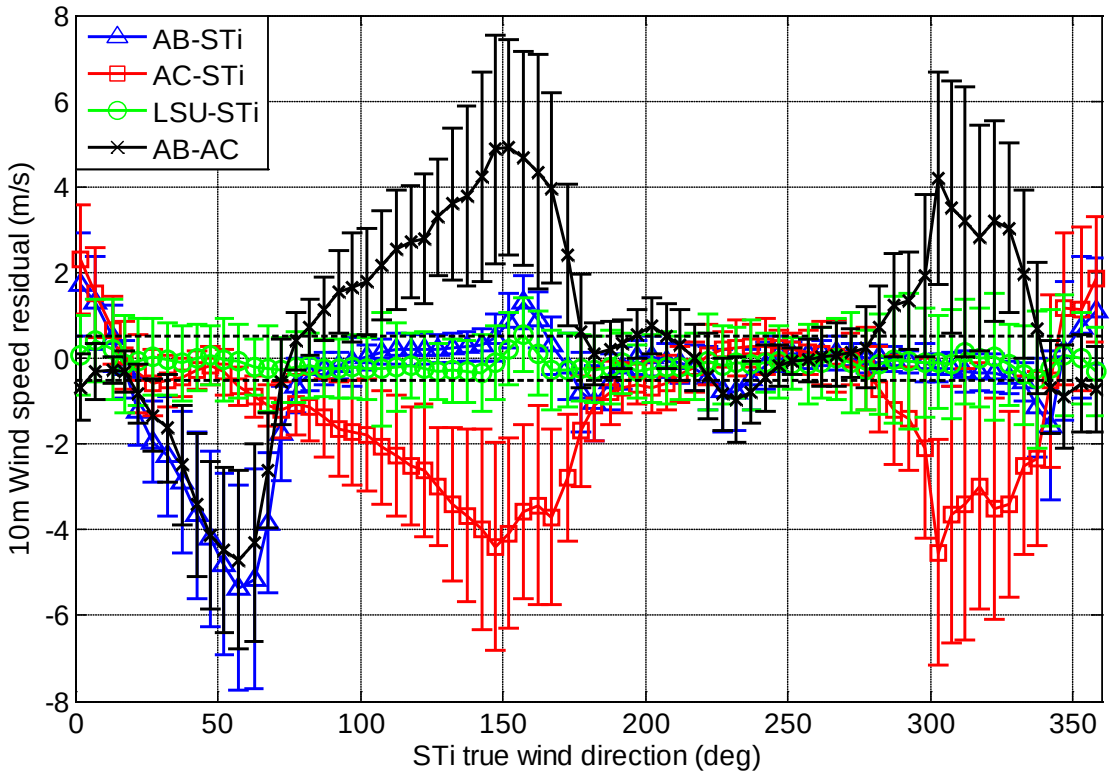

Figure 9. Wind speed residuals as a function of STI wind direction (1 m/s bins). The horizontal dash lines indicate +/- .5m/s.

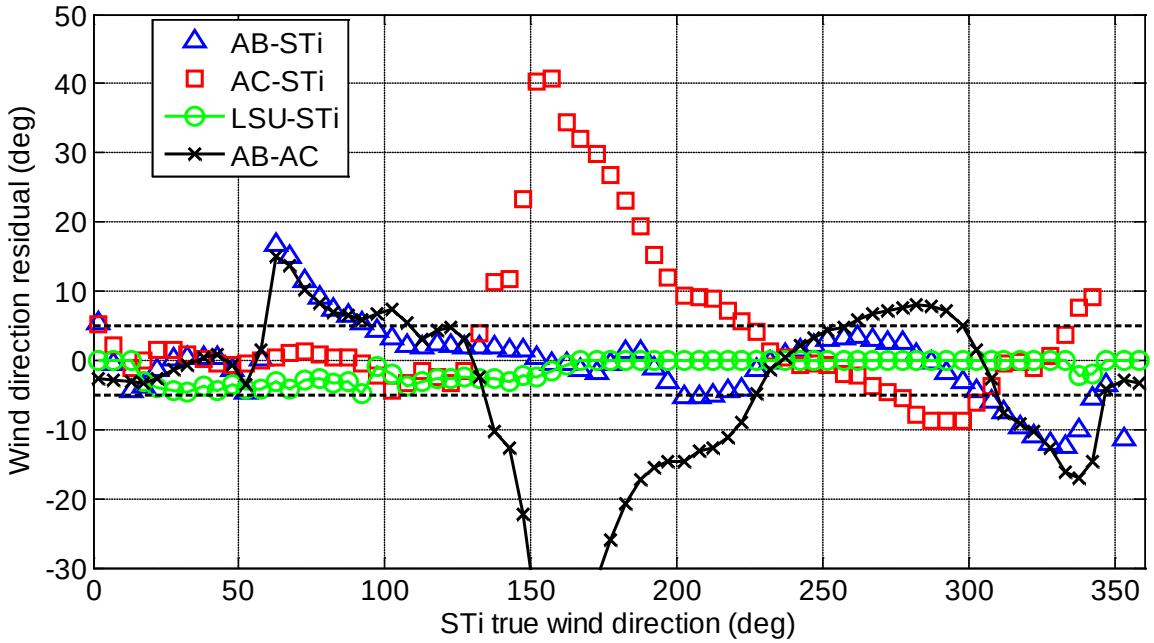

Figure 10. Wind direction residuals as a function of STI wind direction (5 deg bins). The horizontal dash lines indicate +/- .5deg.

5) Quality control and data filtering

In this section, we describe the main criteria used to quality control the flux data set. We start with the wind direction as it is one of the main factors affecting the flux observations due to distortion from the platform structure. Figures 9 and 10 present some of those effects. At about 60 degrees, the wind blows straight into the AC flux package, while at this angle the A structure blocks the AB flux location. At 150 degrees, the wind is blowing straight into the AB location, while the AC flux package is obstructed by the A structure (see Figure 11). This can be observed as deflections in wind directions (Figure 10) and decelerations in wind speeds (Figure 4).

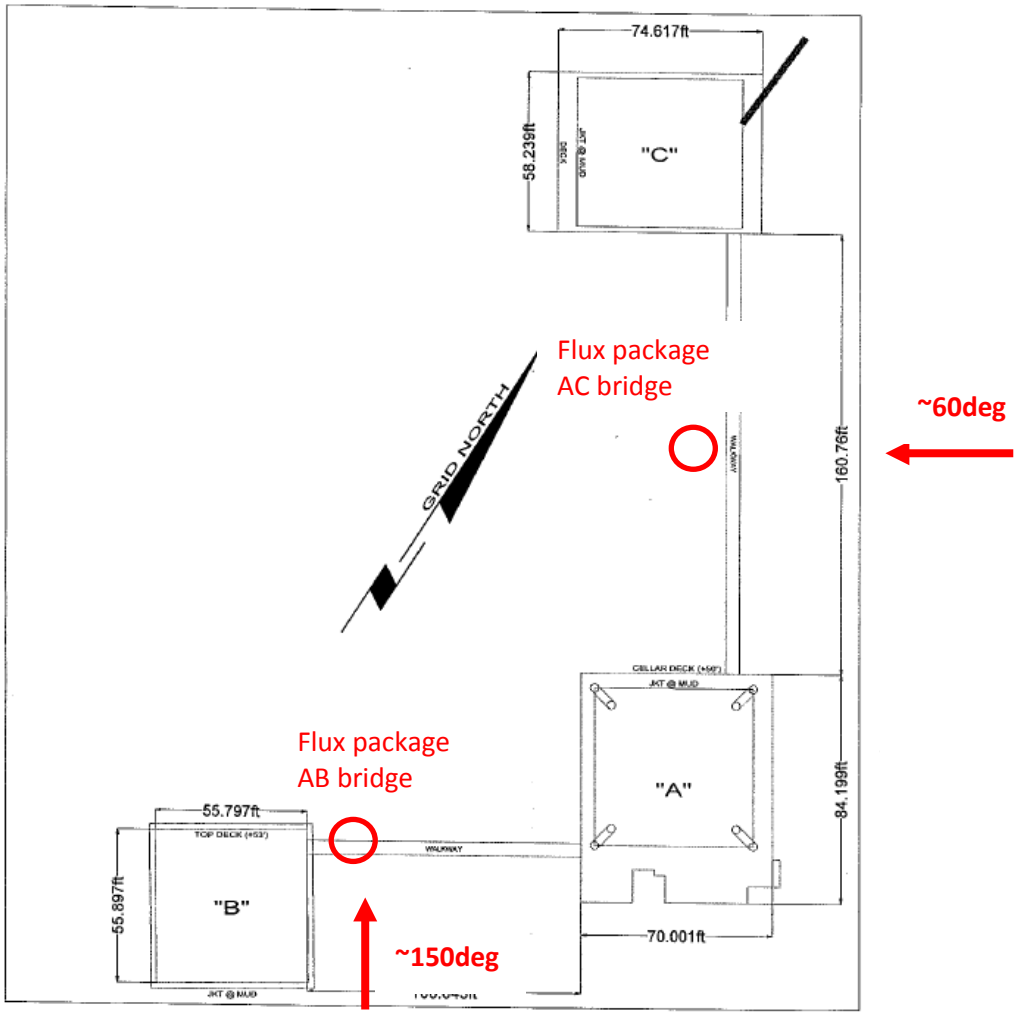

Figure 11. A, B and C structures orientation relative to true North.

Using figures 9, 10 and 11, we selected the following wind sectors as good potential wind directions for flux observations. AB: (80,170), (240,310), AC: (10, 80), (220,280). This results in about 60% of usable data for year of 2011 (combining AB and AC data).

In addition to wind direction criteria, other filters were used to check on reasonable limits on certain other variables. For instance Figure 12 below shows examples of U and W spectra in good wind sector for two different hours. While for a particular hour, the spectra fit well with the $f^{-2/3}$ inertial subrange line (blue and red solid lines), it behaves strangely for a consecutive hour. This could be due to distortion effects or any other reasons affecting high frequencies. To filter out those bad behaviors, we use the inertial dissipation method and computes u*, T*, q* and uses those variables as filters to constrain our direct covariance calculations.

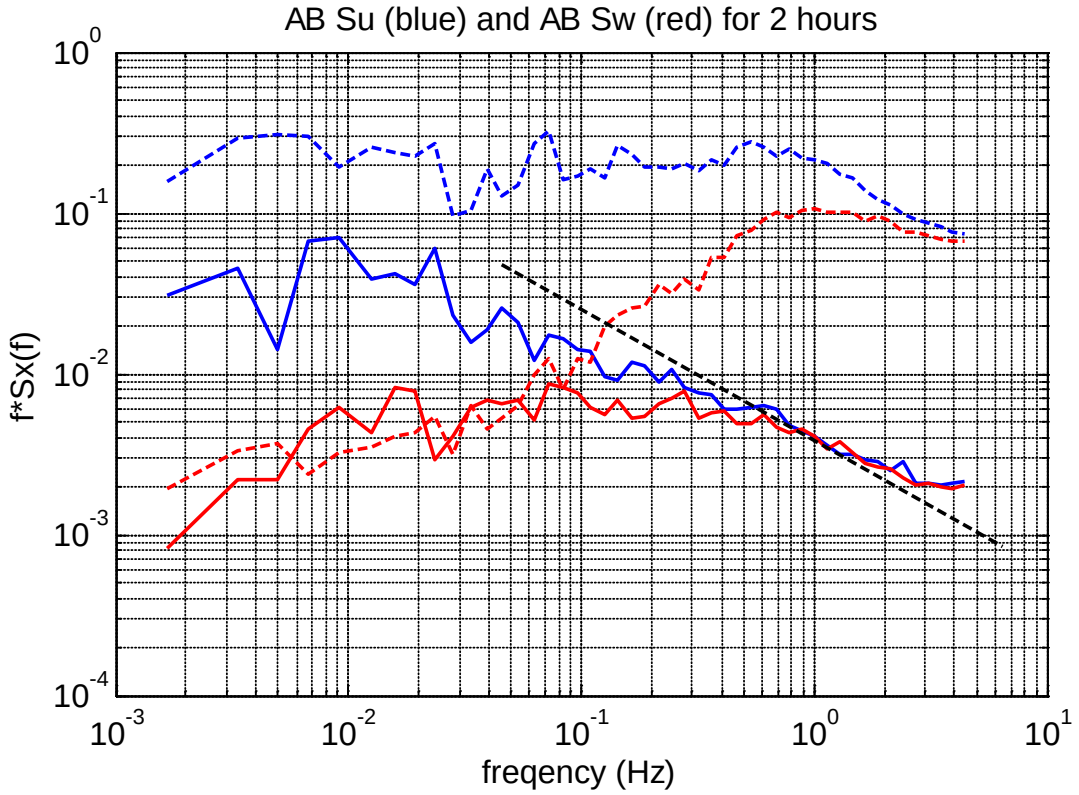

Figure 12. U (blue) and W (red) spectra from the AB flux package for two different hours within the same day. The black dash line indicates a slope of -2/3.

The standard deviations of the 10 Hz data within the ten minute averaging were also used in filtering the data. As an example, the Automatic Gain Control (AGC) of the Licor 7500 was used in complement with other filters to remove bad data or when the optics is cleaned by the automated washing system (see Figure 13).

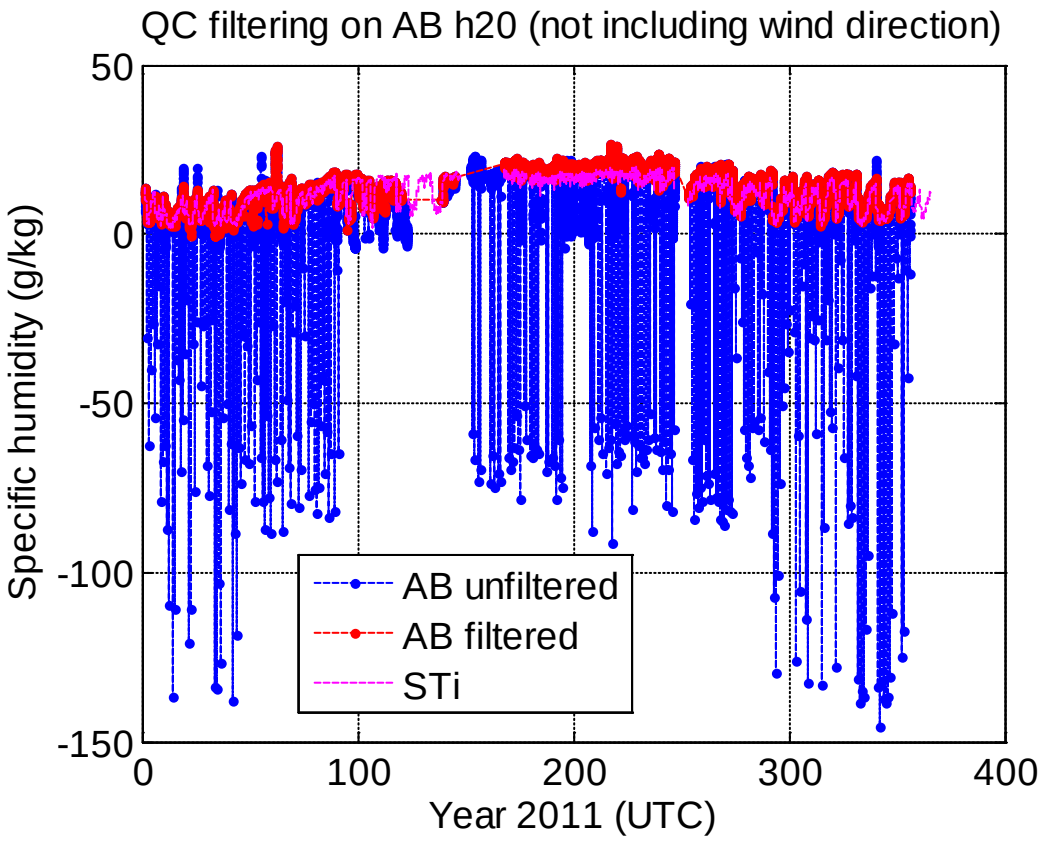

Figure 13. Illustration of unfiltered (blue) and filtered (red) H2) data from the AB Licor 7500 sensor versus the STi unit. No height adjustment done here and no wind direction filtering. The drops are when washing or rain occurs.

6) Direct Covariance against BULK estimates

Bulk estimates of air sea fluxes were computed using the COARE bulk algorithm version 3.0 (Fairall et al., 2003). Cool skin and warm-layer corrections were applied within the algorithm to correct the measured sea temperature to interfacial temperature. Direct wave measurements were not used in the code at that point. Direct covariance latent heat fluxes have been corrected for the density Webb effect and when computing the sensible heat flux, the humidity contribution to sonic temperature was removed using the bulk latent heat flux. No other corrections were applied for that comparison. After applying all correction and filtering, about 50% (180 days) of the data in year 2011 remained.

Figures 14, 15 and 16 show comparison plots for edited stress, sensible heat, and latent heat flux measured in year of 2011. We notice in all three types of fluxes that the covariance measurements are significantly lower than the BULK estimates. Several possibilities have been investigated but no physical reasons have yet explained the differences. Below we comments on the possibilities that remain to be understood:

- the BULK met data inputs need to be further evaluated and post-calibrated to reduce the uncertainty in the BULK flux estimate. Moreover wave and SST effects (cool skin/warm layer) need to be closely looked at to see their effects on flux estimates in that region.
- no obvious flow distortion effects were eminent yet but we so far have looked at flow tilt limits or wind speed/direction (by comparing with other nearby platforms). However this relates to mean state variables and the turbulence variables could behave differently. Flow distortion is more of a concern for stress rather than sensible and latent heat flux.
- additional correction can be applied to the latent heat flux (Licor specific humidity). At that point we decided not to apply any adjustment but after post-calibration this is something to look at. The Licor 7500 signal has higher mean humidity (~10-15%) and perhaps scaling the turbulent fluctuations with the mean ratio of the Licor humidity to the STi humidity will help reduce the discrepancies between BULK and covariance latent heat flux.
- Those discrepancies could also be real and showing that the COARE algorithm needs to be refined for this particular study. Perhaps investigating offshore flow versus inland flow might help elucidate some of the differences, and comparing with other instruments on the platform might be beneficial as well (microwave radiometer, sonar, etc…).

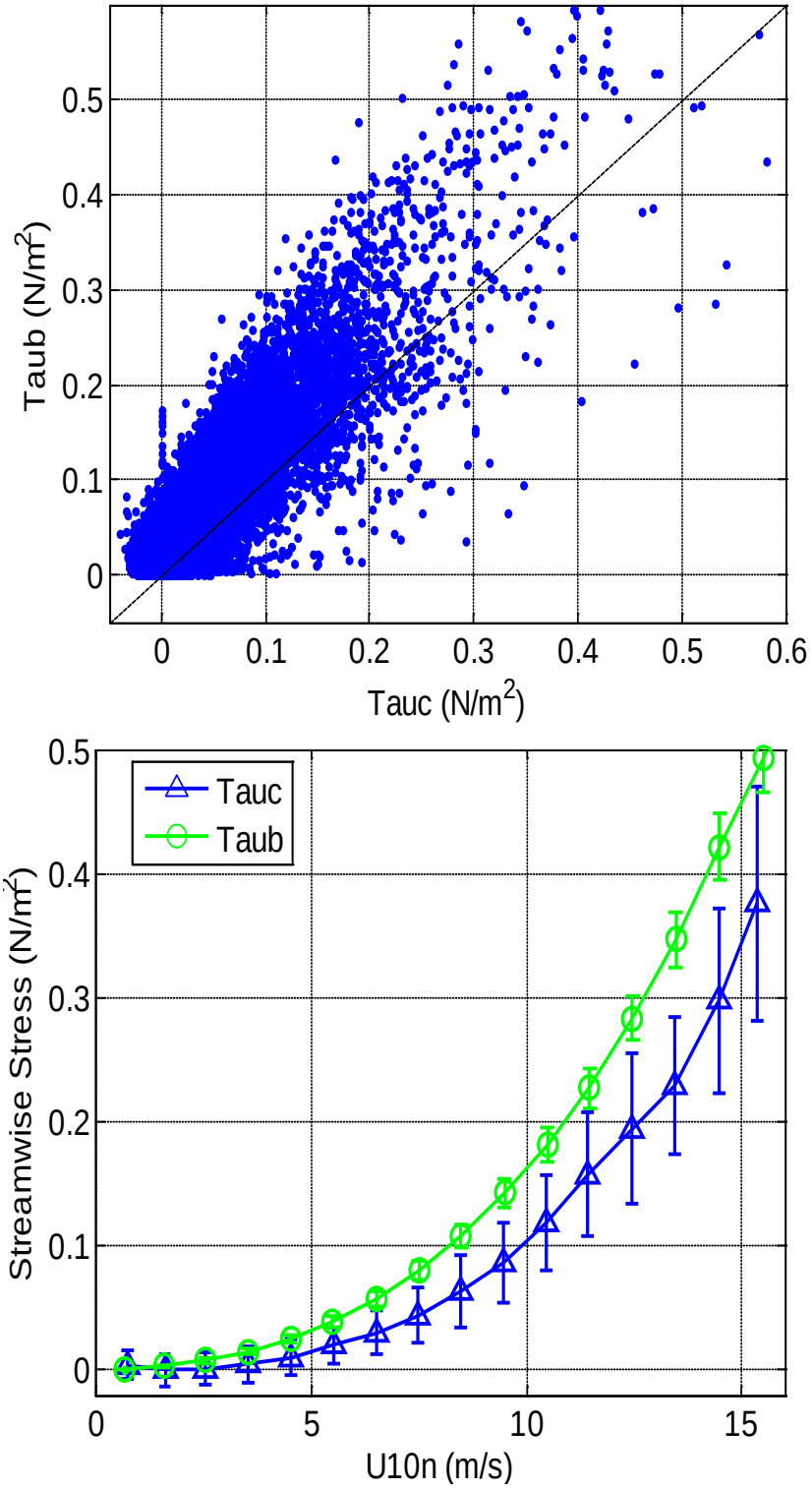

Figure 14. Top panel: BULK stress (Taub) versus measured streamwise stress (Tauc). Lower panel: same flux but bin averaged and plotted as a function of 10-m neutral wind speed.

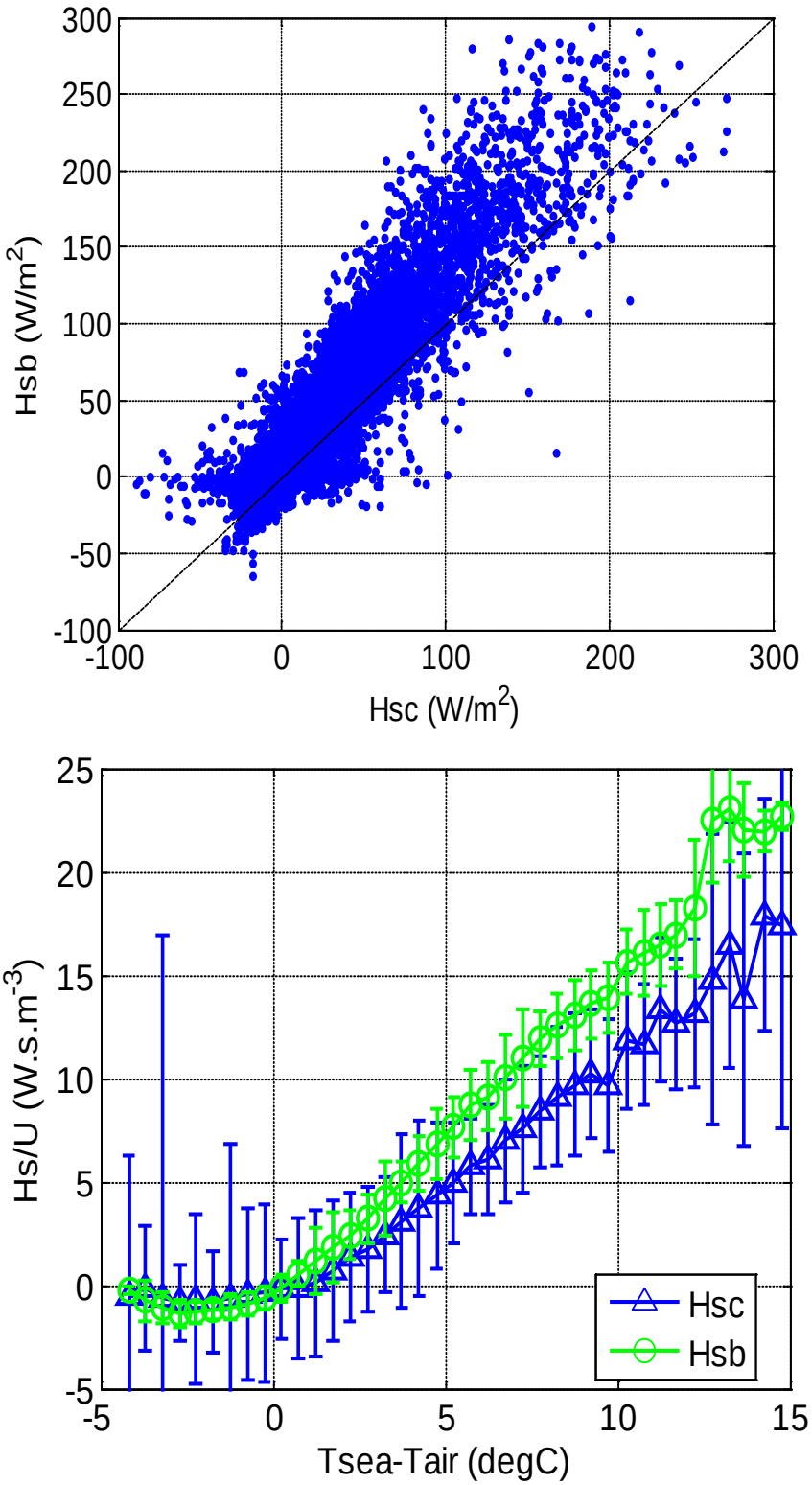

Figure 15. Top panel: BULK sensible heat flux (Hsb) versus measured sensible heat flux (Hsc). Lower panel: same flux but divided by wind speed and plotted as a function of sea-air temperature difference.

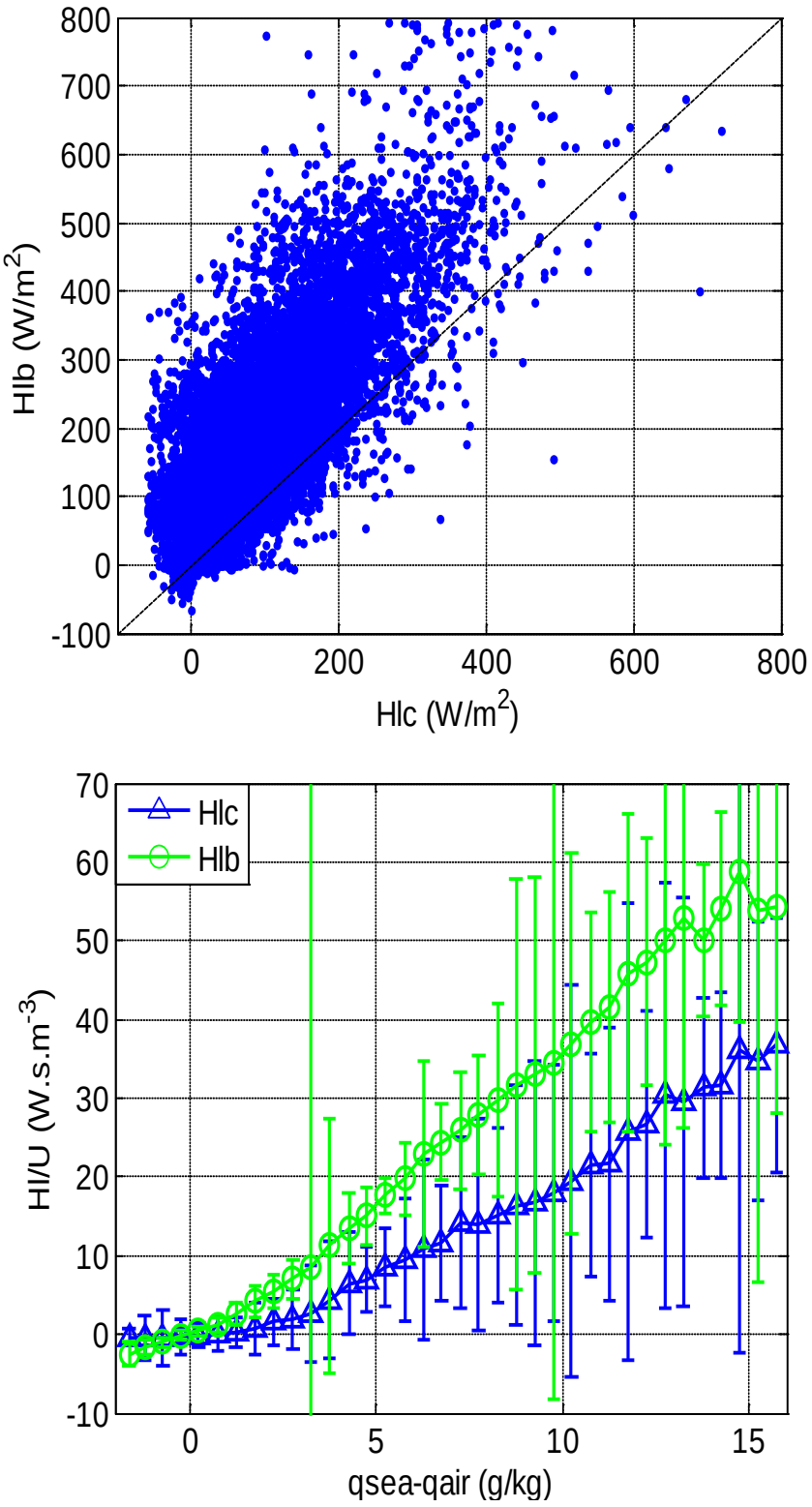

Figure 16. Top panel: BULK latent heat flux (Hlb) versus measured latent heat flux (Hlc). Lower panel: same flux but divided by wind speed and plotted as a function of sea-air specific humidity difference.

7) Conclusion

A limited analysis comparing the COARE flux estimates with direct measurements has been performed for data collected from the ST-52B oil platform. Results show discrepancies between the BULK and covariance fluxes and have yet to be understood. Are the differences simply due to the platform distortion effects, or is it real and do we need to retune the COARE algorithm to the Gulf of Mexico region? Are the measurements at 40m even in the surface layer? What about offshore versus inshore influences? Once the mean surface observations are verified and the COARE algorithm options fully evaluated (wave effects), the user of this data set can address those questions.

To access the current data set: ftp://ftp1.esrl.noaa.gov/psd3/cruises/STIplatform_ST52/flux/Processed/ Data for year *yyyy* are saved in the ASCII file *ST52_10minflux_yyyy.r1*. The files are 60 columns and can be directly acquired with a simple 'load' statement in Matlab.

```
x=load('your_local_directory\ST52_10minflux_yyyy.r1');%read file with 10min-average data;
```

The columns assignment is as follow:

```
year=x(:,1);%year
jdy=x(:,2);%day-of-year at beginning of time average
lat=x(:,3);%latitude (deg)
lon=x(:,4);%longitude (deg)
STi_ta=x(:,5);%air temperature, STi (C)
STi_tsea=x(:,6);%sea temperature, STi floating thermistor 20cm depth (C)
STi_spd=x(:,7);%true wind speed, STi (m/s)
STi_dir=x(:,8);%true wind direction, STi (deg)
STi_qa=x(:,9);%air specific humidity, STi (g/kg)
STi_qse=x(:,10);%sea surface specific humidity from floating thermistor (g/kg)
STi_rs=x(:,11);%downward solar flux, STi (W/m^2)
STi_rl=x(:,12);%downward IR flux, STi (W/m^2)
press=x(:,13);%barometric pressure (mb)
zu_STi =x(:,14);%height of mean wind sensor, STi (39.98 m)
zt_STi =x(:,15);%height of mean air temperature sensor, STi (39.27 m)
LSU_ta=x(:,16);%air temperature, LSU (C)
LSU_tsea=x(:,17);%sea temperature, LSU 1m depth near-surface sensor (C)
LSU_spd=x(:,18);%true wind speed, LSU (m/s)
LSU_dir=x(:,19);%true wind direction, LSU (deg)
LSU_qa=x(:,20);%air specific humidity, LSU (g/kg)
LSU_qse=x(:,21);%sea surface specific humidity from LSU sensor (g/kg)
zu_LSU =x(:,22);%height of mean wind sensor, LSU (39.98 m)
zt_LSU =x(:,23);%height of mean air temperature sensor, LSU (39.57 m)
AB_spd =x(:,24);%unedited true wind speed, AB sonic (m/s)
AB_dir =x(:,25);%unedited true wind direction, AB sonic (deg)
AB_taucx =x(:,26);%unedited covariance streamwise stress, AB sonic (N/m^2)
AB_taucy =x(:,27);%unedited covariance cross-stream stress, AB sonic (N/m^2)
AB_taucx_flag =x(:,28); %QC flag for AB covariance stress. If equal 1, data are
bad or suspicious.
AC_spd =x(:,29);%unedited true wind speed, AC sonic (m/s)
AC_dir =x(:,30);%unedited true wind direction, AC sonic (deg)
```

```
AC_taucx =x(:,31);%unedited covariance streamwise stress, AC sonic (N/m^2)
AC_taucy =x(:,32);%unedited covariance cross-stream stress, AC sonic (N/m^2)
AC_taucx_flag =x(:,33); %QC flag for AC covariance stress. If equal 1, data are
bad or suspicious.
tauxcov=x(:,34);%edited covariance streamwise stress, AB and AC sonic combined
(N/m^2)
taub =x(:,35);%unedited bulk wind stress along mean wind, (N/m^2)
AB_tson=x(:,36);%unedited sonic temperature, AB sonic (C)
AB_hsc=x(:,37);%unedited covariance sensible heat flux, AB sonic (W/m^2)
AB_hsc_flag=x(:,38); %QC flag for AB covariance sensible heat flux. If equal 1,
data are bad or suspicious.
AC_tson=x(:,39);%unedited sonic temperature, AC sonic (C)
AC_hsc=x(:,40);%unedited covariance sensible heat flux, AC sonic (W/m^2)
AC_hsc_flag=x(:,41); %QC flag for AC covariance sensible heat flux. If equal 1,
data are bad or suspicious.
Hscov =x(:,42); %edited covariance sensible heat flux, AB and AC sonic combined
(W/m^2)
Hsb =x(:,43);%unedited bulk sensible heat flux, (W/m^2)
AB_H2O=x(:,44); %air specific humidity, AB Licor (g/kg)
AB_hlc=x(:,45);%unedited covariance latent heat flux, AB (W/m^2)
AB_hlc_flag=x(:,46); %QC flag for AB covariance latent heat flux. If equal 1,
data are bad or suspicious.
AC_H2O=x(:,47); %air specific humidity, AC Licor (g/kg)
AC_hlc=x(:,48);%unedited covariance latent heat flux, AC (W/m^2)
AC_hlc_flag=x(:,49); %QC flag for AC covariance latent heat flux. If equal 1,
data are bad or suspicious.
Hlcov =x(:,50);%edited covariance latent heat flux with Webb et al. correction,
AB and AC combined (W/m^2)
Hlb=x(:,51);%unedited bulk latent heat flux, W/m^2 (includes Webb et al.
correction)
hl_webb=x(:,52);%correction to measured latent heat flux, Webb et al.
zu_son0=x(:,53);%height of AB sonic, 11 m
zu_son1=x(:,54);%height of AB sonic, 14 m
AB_CO2=x(:,55);% CO2 concentration, AB Licor (umol/mol)
AB_wCO2=x(:,56);% LICOR CO2 flux, AB Licor (micatm m/s)
AB_wCO2_flag=x(:,57); %QC flag for AB covariance CO2 flux. If equal 1, data are
bad or suspicious.
AC_CO2=x(:,58);% CO2 concentration, AC Licor (umol/mol)
AC_wCO2=x(:,59);% LICOR CO2 flux, AC Licor (micatm m/s)
AC_wCO2_flag=x(:,60);%QC flag for AC covariance CO2 flux. If equal 1, data are
bad or suspicious.
```

References

Fairall, C. W., E. F. Bradley, J. E. Hare, A. A. Grachev, and J. B. Edson, 2003: Bulk parameterization of air-sea fluxes: Updates and verification for the COARE algorithm. J. Climate, 16, 571-591.